Hot-Ion Effects and Mode Conversion of the Lower-Hybrid Wave

G. A. Wurden,[a] K. L. Wong, F. Skiff, and M. Ono
Plasma Physics Laboratory, Princeton University, Princeton, New Jersey 08544
(Received 27 December 1982)

Finite-ion-Larmor-radius modification of lower-hybrid waves in the ACT-1 toroidal plasma at frequencies $\omega \simeq (4-8)\omega_{ci}$, close to the lower-hybrid resonance layer, is observed experimentally. Probe and CO_2 laser scans of the wave amplitude show patterns at frequencies above each ion cyclotron harmonic. Modeling with a hot-ion, electrostatic-ray-tracing code and Fourier reconstruction of the wave form provide evidence for linear mode conversion to hot-plasma waves.

PACS numbers: 52.35.Fp, 52.40.Db, 52.50.Gj

Lower-hybrid waves (LHW) are of importance to ion and electron heating as well as to driving of toroidal currents in tokamak fusion devices. Linear mode conversion of LHW into hot-plasma waves (HPW) and then ion Bernstein waves (IBW) as the LHW approaches the lower-hybrid resonance layer from the low-density side was predicted theoretically by Stix[1] in 1965, and sketched for a single parallel wave number $k_\parallel$. In 1969, Fisher and Gould[2] showed experimentally that LHW propagate in resonance cones when a spread in $k_\parallel$ is launched from an antenna. Since that time, a number of authors[3-6] have suggested that resonance cones from a localized source antenna are maintained throughout the mode-conversion processes. This idea has influenced experimental searches for LHW → HPW mode conversion, none of which have reported success.[7] However, in a manner analogous to (but more complicated than) finite electron temperature's causing well-known dispersion and interference effects,[8] the inclusion of finite ion temperature in a magnetized plasma causes extensive spatial dispersion and interference structures in the wave packet of the original LHW near the LH resonance layer. As has been pointed out by Simonutti,[9] a key signature of the mode-conversion processes would be a periodicity of wave forms in the parameter $\eta = \omega/\omega_{ci}$, where ω_{ci} is the local ion cyclotron frequency, and $f = \omega/2\pi$ is the launching frequency from the antenna.

In this Letter, we report the first experimental observation of finite-ion-Larmor-radius modifications of lower-hybrid waves, characterized by ion-cyclotron periodicity, in close vicinity ($1 \lesssim \omega/\omega_{1h} < 2$) to the lower-hybrid layer $\omega_{1h} = \omega_{pi}(1 + \omega_{pe}^2/\omega_{ce}^2)^{-1/2}$, where ω_{pi}, ω_{pe}, and ω_{ce} have the usual definitions as the ion plasma, electron plasma, and electron cyclotron frequency, respectively. Mode conversion of the lower-hybrid wave to hot-plasma waves is required to calculate patterns observed in the data, with the experimentally determined radial electron density, ion temperature, electron temperature, toroidal magnetic field profiles, and ion concentration information as input parameters.

This experiment was performed in the Princeton Advanced Concepts Torus (ACT-1) steady-state toroidal plasma device[10] at frequencies $\omega \sim (4-8)\omega_{ci}$, or $f \sim 25-50$ MHz, with $n_e \sim (2-8) \times 10^{10}$ cm^{-3}, $T_i \sim 0.5-2$ eV, $T_e \sim 0.5-3$ eV, $B_0 \simeq 4.5$ kG, and parallel wavelengths launched by the antenna covering the range $\lambda_\parallel \sim 2-20$ cm. The antenna structure consisted of six narrow (width $\Delta z = 0.65$ cm) plates on 1.3-cm centers located on the outer major radius edge of the plasma at a midplane minor radius of $r = 6.5$ cm, protected by limiters at $r = 6$ cm. Only one of the central plates was powered (less than 0.1 W to avoid nonlinear effects[11]), resulting in a broad $k_\parallel$ spectrum and waves launched in both directions around the torus. The filament-produced hydrogen plasma consisted of H_1^+, H_2^+, and H_3^+, in the ratio $0.45 : 0.27 : 0.28 \pm 0.05$, measured by ion cyclotron wave resonance cone techniques.[12] Radial ion temperature information was obtained via second-harmonic ion Bernstein wave measurements, using rf probes and CO_2 laser scattering.[13] Radial electron density profiles, measured from high-frequency ($\omega \gg \omega_{1h} \simeq \omega_{pi}$) lower-hybrid resonance-cone angles and Langmuir-probe traces, complete the basic plasma parameters.

ACT-1 differs from older devices[7] with regrad to LHW studies in four important respects. The ion temperature is higher, so that waves with $k_\perp \rho_i \sim 0.5-2$, where ρ_i denotes the ion Larmor radius, are readily obtained. Long effective machine lengths are achieved (a torus) so that the wave can approach the resonance layer along weak gradients in the perpendicular (radial or x) direction, with no gradients in the parallel direction. Since the plasma source is in the inner

half of the torus, fast electrons (by the nature of their vertical drifts) are effectively isolated from the observation region, and thus electron Landau damping on a superthermal tail is not a problem.[14] Finally, the toroidal magnetic field (there is no poloidal field) falls off as one over the major radius, so that the wave is launched into a plasma with $\nabla_x n \cdot \nabla_x B > 0$, usually encountering one to two cyclotron harmonic layers before reaching the axis.

In Fig. 1, probe signals of wave amplitude versus radius, obtained using a tuned spectrum analyzer as a narrow-band filter, are plotted as a function of launching frequency. The probe was 9 ports (26 ports ~ 360°) away from the antenna toroidally. The largest feature on each trace is the resonance cone from the short way around the torus, while features closer to $r = 0$ cm have come from the long way around the torus. The most interesting data, pointed out by arrows, are near 32–34, 40–41, and 48 MHz. Wave amplitude is seen to pile up in front of the fifth, sixth, and seventh ion cyclotron layers (denoted by diagonal lines). Interference patterns, changing dramatically for frequency differences of only 0.25 MHz, appear with cyclotron periodicity. These patterns are very sensitive to small changes in plasma parameters or magnetic field, and also appeared on wave interferometry probe traces. At $f = 32$ MHz, the bump near $r = 2$ cm corresponds to $f/f_{pi} \simeq 1.1$, while at $f = 40.5$ MHz, the sharp feature at $r = 1$ cm corresponds to $f/f_{pi} \simeq 1.2$. Finally, broadening of the main cone is visible near each harmonic layer.

When examined with CO_2 laser scattering, which selectively detects different $k_\perp$, similar periodicity was observed. Phase velocity was consistent with a backward wave propagating into the plasma, or a forward wave propagating out of the plasma. The $k_\perp$ detected ranged from 25 to 60 cm^{-1}. Coherence problems prevented seeing $k_\perp > 60$ cm^{-1} at the low power levels required to avoid perturbing the plasma.

It can be deduced from Fig. 2(a), which shows calculated $k_\perp$ versus radius at $f = 41$ MHz for

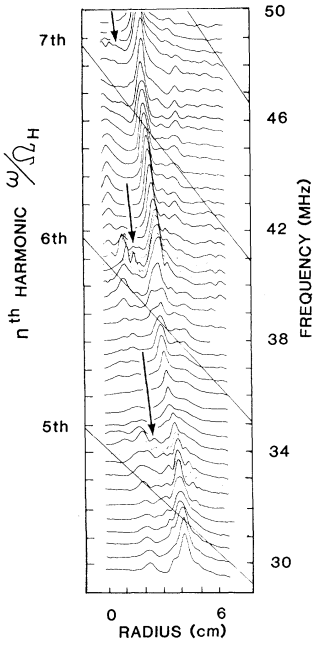

FIG. 1. Radial probe scans of wave amplitude as a function of applied rf frequency, ~120° toroidally from the antenna, which was located radially at $r = 6.5$ cm. Interference patterns can be seen in bands above ion cyclotron harmonics, as well as distortion and broadening of the resonance cone (main feature) near each harmonic layer. The innermost features are from waves traveling the long way around the torus.

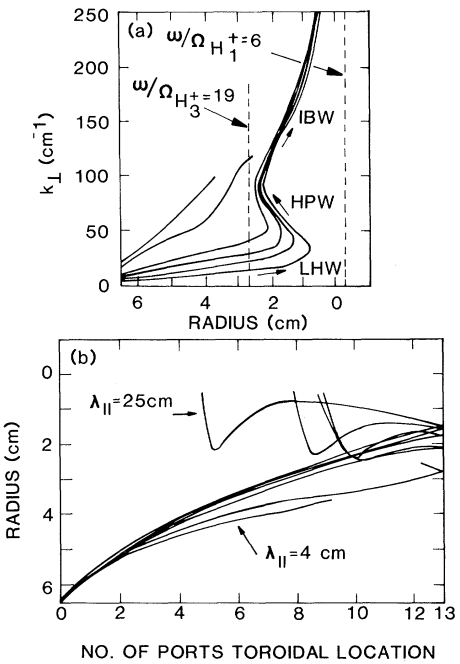

FIG. 2. Ray-tracing code results using experimental plasma parameters, for $\lambda_\parallel = 4$, 5, 9, 12, 15, and 25 cm at $f = 41$ MHz (13 ports = 180° around the torus). (a) Perpendicular wave number k_x vs radial position. The shortest $\lambda_\parallel$ are heavily electron Landau damped, while longer-$\lambda_\parallel$ modes convert from LHW→HPW→IBW, which are then ion-cyclotron damped in front of the sixth harmonic layer. (b) Corresponding ray-tracing trajectories. The characteristic "hook" pattern formed by outgoing hot-plasma waves and inward propagating ion Bernstein waves is evident.

various $\lambda_{\parallel}$, that to directly detect the mode-converted HPW, $k_{\perp}$ should be in the range of 40–100 cm^{-1}. The Bernstein wave should exist even higher, $k_{\perp} \sim 100$–200 cm^{-1}. It is evident that the laser data alone cannot distinguish conclusively between HPW and LHW of differing $\lambda_{\parallel}$ with the same $k_{\perp}$. However, to explain the probe data, which cannot be generated by LHW alone, requires that LHW interfere with HPW to produce the observed patterns. This is suggested by corresponding ray-tracing results shown in Fig. 2(b), where it can be seen that mode conversion to the HPW and IBW breaks up the initial resonance cone, since the LHW → HPW conversion points for different $\lambda_{\parallel}$ are at widely differing toroidal and radial locations. Since the hot-plasma-wave region is defined between the two turning points (LHW → HPW and HPW → IBW), the latter of which depends strongly on proximity to an ion cyclotron harmonic layer, strong magnetic field dependence is expected.

In order to simulate the probe data to see if such interference patterns could in fact be generated, a computer code was written to reconstruct the radial profile of the rf electric field amplitude, $E_{\perp}(x,z)$. The antenna $k_{\parallel}$ spectrum (each component $A_{k_{\parallel}}$) is assumed to be given, and in fact has been estimated with the laser scattering system. For this two-dimensional problem, eighty $k_{\parallel}$ components, centered in a Gaussian about $k_{\parallel} = 0.9$ cm^{-1}, are numerically propagated into the plasma in the Wentzel-Kramers-Brillouin (WKB) sense:

$$E_{k_{\parallel}}(x) = A_{k_{\parallel}} \exp(i \int_0^x k_{\perp}(k_{\parallel}, x')dx') |k_{\perp}(x)|^{1/2}.$$

Here $k_{\perp}$ (complex) is obtained by finding a root of the hot-ion electrostatic dispersion relation, given the magnetic field, plasma parameter profiles, and $k_{\parallel}$. Electromagnetic effects are unimportant, and can be ignored for ACT-1 parameters.[15] At points of mode conversion, where $dx/dk_{\perp} = 0$, the WKB approximation clearly fails.

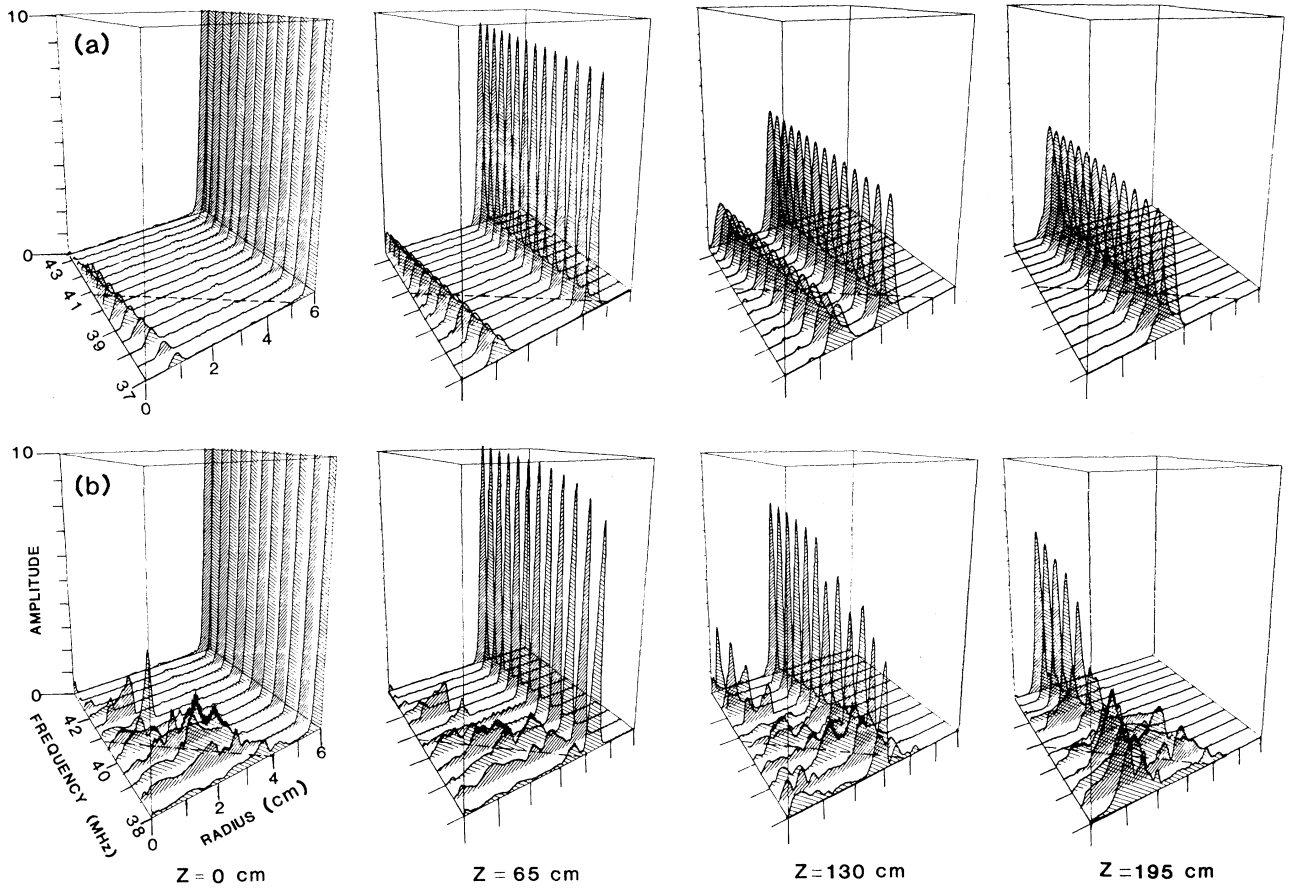

FIG. 3. Fourier reconstruction code results of wave-form amplitudes for a range of launching frequencies, at four toroidal distances from the antenna for (a) cold ions and (b) hot ions. $T_i = 0.5$ eV at $r = 6$ cm plasma edge, increasing linearly to $T_i = 2$ eV at $r = 0$ cm, on axis.

However, these regions are very narrow for ACT-1, and although phase errors are introduced because the exact connection problem has been neglected, the general picture is not significantly altered. The total electric field is then obtained by the Fourier sum over $k_{\parallel}$.

Electric field amplitude calculated from this code is shown in Fig. 3(a) for cold ions, and Fig. 3(b) for hot ions ($T_i = 0.5$ eV edge, 2 eV center), with all other parameters fixed, for a set of launching frequencies. Four toroidal locations, ranging from $z = 0$ cm (at the antenna toroidal position) to $z = 195$ cm (~ halfway around the machine), are depicted. Wave amplitude in Fig. 3(b) is seen to "track" the harmonic layer, represented by the dashed line $\omega/\omega_{ci} = 6$, in a fashion very similar to the experimental data shown in Fig. 1. In particular, sharp interference structures can be seen which move through the "main cone" near the harmonic layer, as well as damping of the cone near the harmonic layer in the hot-ion case. Mode-converted HPW are responsible for features outside of, and at some frequencies on top of, the resonance-cone remnants. These effects are absent for cold ions or unmagnetized ions.

In summary, the presence of a modification of the lower-hybrid wave trajectory, characterized by ion-cyclotron periodicity, has been seen experimentally for the first time. We have shown that this feature is reproduced theoretically when mode conversion to the hot-plasma wave with magnetized ions is taken into account. In a large tokamak LHW experiment, such as on the Princeton Large Torus, the wave frequency is $f \simeq (20-40) \times f_{ci}$. But at the same time $k_{\perp}\rho_i$ is approximately five times larger than in ACT-1, so that similar effects should be present. However, because of the presence of a poloidal field and many closely spaced harmonic layers, the effects may be subtle and difficult to observe directly.

The authors would like to thank J. Taylor and W. Kineyko for their invaluable technical support, and T. Stix and V. Decyk for useful discussions. This work is funded by U. S. Department of Energy Contract No. DE-AC02-76-CH0-3073. One of us (F. S.) acknowledges receipt of a Fannie and John Hertz Foundation Fellowship.

[a]Present address: Los Alamos National Laboratory, Los Alamos, New Mexico 87545.

[1]T. H. Stix, Phys. Rev. Lett. 15, 878 (1965).

[2]R. K. Fisher and R. W. Gould, Phys. Rev. Lett. 22, 1093 (1969).

[3]P. M. Bellan and M. Porkolab, Phys. Fluids 17, 1592 (1974).

[4]H. H. Kuehl and K. K. Ko, Phys. Fluids 18, 1816 (1975).

[5]M. Porkolab, Phys. Fluids 20, 2058 (1977).

[6]C. L. Grabbe, Phys. Fluids 22, 1323 (1979).

[7]P. M. Bellan and M. Porkolab, Phys. Fluids 19, 995 (1975).

[8]H. H. Kuehl, Phys. Fluids 16, 1311 (1973).

[9]M. D. Simonutti, Phys. Fluids 18, 1524 (1975).

[10]K. L. Wong, M. Ono, and G. A. Wurden, Rev. Sci. Instrum. 53, 409 (1982).

[11]K. L. Wong and M. Ono, Phys. Rev. Lett. 47, 842 (1981); also J. R. Wilson and K. L. Wong, Phys. Fluids 25, 675 (1982).

[12]M. Ono, K. L. Wong, and G. A. Wurden, Phys. Fluids 26, 298 (1983).

[13]G. A. Wurden, M. Ono, and K. L. Wong, Phys. Rev. A 26, 2297 (1982).

[14]G. A. Wurden, Ph.D. thesis, Princeton University, 1982 (unpublished).

[15]H. H. Kuehl, IEEE Trans. Plasma Sci. PS-9, 104 (1981).